Mechanical performance of variable stiffness composite plates subjected to multiscale defects

Mechanical Performance of Variable Stiffness Plates Subjected to Multiscale Defects

ALFONSO PAGANI,
ALBERTO RACIONERO SANCHEZ-MAJANO
and IGNACIO SANCHEZ ZARATE

ABSTRACT

Novel manufacturing techniques that have arisen during the last decades have permitted to improve both the manufacturing quality and performance of laminates parts. Despite these improvements, such manufactured parts are not flaw-exempt, since uncertainty in the fabrication processes and in the material properties are still present. At the same time, numerical models that allow to describe the ground truth designs have been developed. Nevertheless, some defects have not been studied yet. This work aims to analyze the influence of spatially varying microscale defects on the mechanical performance of variable stiffness plates at both microscale and macroscale level. Attention has been paid to the usage of component-wise and layer-wise modeling, based on the Carrera Unified Formulation, to study the stochastic response of the micromechanical stresses and the macroscale buckling performance, respectively.

Alfonso Pagani, Mul2 Group, Politecnico di Torino. Corso Ducca degli Abruzzi 24, Turin, Turin 10129, Italy.
Alberto R. Sanchez-Majano, Mul2 Group, Politecnico di Torino. Corso Ducca degli Abruzzi 24, Turin, Turin 10129, Italy.
Ignacio S. Zarate, Mul2 Group, Politecnico di Torino. Corso Ducca degli Abruzzi 24, Turin, Turin 10129, Italy

INTRODUCTION

Automated fabrication techniques, such as Automated Fiber Placement (AFP) [1], have broadened the manufacturing possibilities of laminated structures. Apart from improving the quality of the produced parts, new families of composites have been conceived, namely Variable Angle Tow (VAT) composites. Such structures broaden the design space thanks to their capabilities of redistributing the stresses to desired regions, which may allow weight reduction.

However, every manufacturing process is subjected to the uncertainty that arises from different factors. Uncertainty in the micromechanical properties can be one of those. Recent works have addressed this phenomenon. For instance, Dey *et al.* [2] imposed uncertainty in the material elastic properties at the micro and macroscale level. It was demonstrated that considering such stochasticity at the microscale broadens the stochastic structural response.

There exist several fashions in which randomness in material properties, laminae thickness, etc., can be imposed. During the last years, stochastic fields [3] have been used to impose variability. These fields are commonly generated by means of the Karhunen-Loève Expansion (KLE) [4] thanks to their capabilities of combining them with metamodeling techniques. For instance, Guimaraes *et al.* [5] used KLE to generate variability in the fiber volume fraction (FVF) of tow-steered composite plates. Moreover, they employed Polynomial Chaos Expansion (PCE) [6] as regression metamodel to compute aeroelastic sensitivity statistics.

In this manuscript, Carrera Unified Formulation (CUF) [7] is used to model VAT plates. CUF has been used to analyze a variety of mechanical problems, such as micromechanics [8], rotor dynamics [9], and hygrothermal analyses [10]. In recent years, CUF has also been extended to the analysis of VAT plates, as shown in the papers by Vescovini and Dozio [11] and Viglietti *et al.* [12]. Additionally, manufacturing-induced mesoscale uncertainty on VAT components has been studied in [13] and [14]. Following this research path, this work aims to investigate how microscale uncertainty propagates through the scales of VAT laminates and how this uncertainty affects the microscale stresses, as well as macroscale stresses and the structural buckling response.

The manuscript is organized as follows: (i) first, a description of the high-order finite elements is made; (ii) then, uncertainty modeling and quantification procedures are depicted; (iii) afterward, the results are gathered and explained; (iv) finally, some concluding remarks are included.

UNIFIED FINITE ELEMENTS

In the framework of CUF [7], the 3D field of displacements can be expressed as a summation, following Einstein notation, of arbitrary expansion functions $F_\tau(x,z)$ and the vector of the generalized displacements $\boldsymbol{u}_\tau(y)$. In the case of one-dimensional beam theories, as in the case of this work, the displacements field is expressed as:

$$\boldsymbol{u}(x,y,z) = F_\tau(x,z)\boldsymbol{u}_\tau(y) \quad \tau = 1,\dots,M \tag{1}$$

where M is the number of expansion terms. Several families of expansion functions can be utilized as $F_{\tau}(x,z)$, being the most common the Taylor expansion (TE), Lagrange expansion (LE), and Hierarchical Legendre expansion (HLE). The last two expansions are the ones used in this work to describe, respectively, the macroscale structure and the microscale UC. In this fashion, a layer-wise (LW) approach is used to analyze the laminated parts. For the micromechanics, a component-wise (CW) approach is obtained by coupling HLE with the blending function method (BFM) [15] to precisely describe the geometry of the curved boundaries present in the micromechanical model.

The Finite element method (FEM) is then used to study the structures involved in this paper. Therefore, the generalized displacements can be expressed as:

$$\boldsymbol{u_{\tau}}(y) = N_i(y)\boldsymbol{u_{\tau i}} \qquad i = 1, \dots, n_{nodes} \tag{2}$$

in which n_{nodes} is the total number of beam nodes, $N_i(y)$ are the one-dimensional shape functions and $\boldsymbol{u_{\tau i}}$ are the nodal unknowns.

In the extensive literature of CUF, it has been demonstrated that the governing equations that lead to the computation of the equilibrium state can be obtained by adopting an adequate recursive notation for the expansion of the kinematics. In this manner, in the FEM framework, the stiffness arrays can be obtained easily, and the accuracy of the analysis can be fine-tuned opportunely.

In this work, the authors report the explicit equations that allow one to obtain the linear stiffness matrix $\boldsymbol{K}$ by means of the Principle of Virtual Displacements (PVD)

$$\boldsymbol{\delta}(L_{int}) = < \boldsymbol{\delta\varepsilon}^T \boldsymbol{\sigma} > = \boldsymbol{\delta} u_{sj}^T \boldsymbol{k_0^{ij\tau s}} u_{\tau i} \tag{3}$$

where $\boldsymbol{k_0^{ij\tau s}}$ denotes the fundamental nucleus of the linear stiffness matrix, and the $<\cdot>$ operator represents the integral over the volume of the element. Then, the assembled global stiffness array is obtained by looping through the indices i, j, τ, s.

The linearized buckling problem is also analyzed in the present paper. For the sake of brevity, the governing equations of that problem are not reported here, but can be found in [16].

MICROMECHANICAL MODELING

Composite structures can be conceived as an ensemble of microstructures periodically distributed over the structures' volume. In this context, the Representative Unit Cell (RUC) represents the essential building block that contains the necessary information to identify the material properties. An illustration of the RUC is available in Figure 1. The macroscopic properties are defined in the global reference system $\boldsymbol{x} = \{x_1, x_2, x_3\}$, whilst the RUC's local reference frame is denoted by $\boldsymbol{y} = \{y_1, y_2, y_3\}$. Micromechanical analyses can be twofold: (i) first, they can be used to calculate the effective properties of the heterogeneous material represented by the RUC as input of the equivalent homogeneous material properties in the

higher-scale analysis; (ii) retrieve the displacements, strains and stresses fields over the RUC from the outputs of the macroscale structural analysis at particular points.

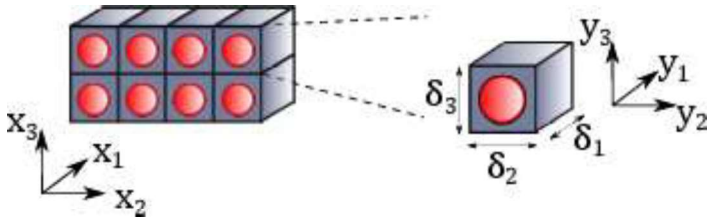

Figure 1. Representation of a period heterogenous material and the associated RUC, along with the global and local reference frames.

Micromechanical analyses assume that the RUC is much smaller than the macroscopic structure, such that $y_i = x_i/\delta$, where δ is a scaling factor that characterizes the dimensions of the RUC. In micromechanics, the material properties provided by the RUC analysis at the microscale are intrinsic properties of the material chosen for the structural analysis. That is, they do not depend on the macroscale structural problem.

In this manuscript, the micromechanical problem is solved by employing the Variational Asymptotic Method (VAM) and the Mechanics of Structure Genome (MSG), initially derived in [17] and [18]. These are then coupled with CUF, as explained in the work by de Miguel [8], to obtain the homogenized material properties of the RUC. For the sake of brevity, the governing equations of the mentioned methods are not reported in this work, but they are available in the cited papers.

UNCERTAINTY MODELLING AND QUANTIFICATION

STOCHASTIC FIELDS

Uncertainty might appear at the different scales of a laminated component. Therefore, it is essential to understand how it affects the mechanical performance of the studied component to enhance the design process. Uncertainty is modeled through stochastic fields generated using the KLE [4] and is included in the numerical model. In this way, a generic two-dimensional random field can be expressed as:

$$H^k(x,y;\boldsymbol{\omega}) = \widetilde{H}^k + \Delta H(x,y;\boldsymbol{\omega}) = \widetilde{H}^k + \boldsymbol{\sigma}_H^k \sum_{i=1}^{\infty} \boldsymbol{\xi}_i(\boldsymbol{\omega}) \boldsymbol{\lambda}_i \boldsymbol{\varphi}_i(x,y) \tag{4}$$

in which $\widetilde{H}^k$ is the mean value of the field, σ_H^k is the field's standard deviation, $\xi_i(\omega)$ are independent Gaussian random variables, and λ_i and $\varphi_i(x,y)$ are the eigenvalues and eigenfunctions solution to a Fredholm integral problem, which depends on the selection of a correlation function $\boldsymbol{\rho}(\boldsymbol{x},\boldsymbol{x}')$. Equation (4) is then truncated up to r terms to generate the random fields. For further knowledge on this topic, the reader is referred to [19].

POLYNOMIAL CHAOS EXPANSION

One of the most used techniques to study stochastic processes is the Monte Carlo (MC) method, in which several parameters, whose influence we want to address, are modified between runs, leading to different results. However, MC is a computationally intensive procedure that requires a vast amount of simulations to provide a good characterization of the desired outcomes. For that reason, numerical techniques such as Polynomial Chaos Expansion (PCE) can be utilized to mitigate the computational cost. Following this surrogate approach, the desired output magnitude $\boldsymbol{\Phi}$ can be expressed in terms of convenient independent variables as:

$$\boldsymbol{\Phi} = \sum_{i=1}^{r} \boldsymbol{\beta}_i \boldsymbol{\psi}_i(\xi_i(\omega)) \tag{5}$$

where $\boldsymbol{\beta}_i$ are the coefficients of the PCE, and $\boldsymbol{\psi}_i(\boldsymbol{\xi}_i(\boldsymbol{\omega}))$ are the orthonormal polynomial set that constitutes the PCE and depends on a set of independent random variables $\xi_i(\omega)$, which are the ones used to generate the stochastic fields. In this manuscript, PCE is used to address the uncertainty regarding the inner stress state and the critical buckling loads. Additional literature concerning PCE can be found in [20].

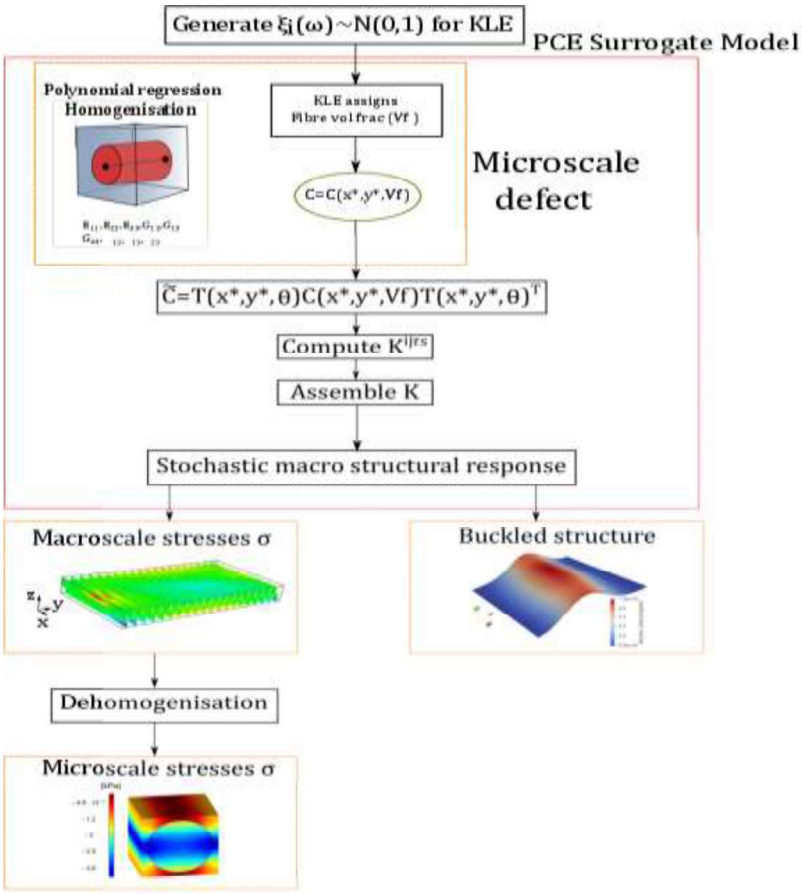

Figure 2. Flow-chart depicting the multiscale uncertainty process.

To conclude this section, a flow-chart explaining how the uncertainty is propagated throughout the scales is shown in Figure 2 and explained herein. First, a set of independent Gaussian random variables is generated in order to obtain the different random fields influencing the laminated structure. These random variables are the input of the FE model. Once the FE simulation is running, a specific value of FVF is assigned to each integration point. The FVF provides the elastic properties of the material by means of polynomial functions that relate, for instance, Young's modulus with the fiber content of the UC. Then, with the elastic properties, the material stiffness matrix is obtained. Afterward, this matrix has to be rotated into the global reference frame of the structure. For doing so, the local fiber orientation is used to compute the rotation matrix, available in the book by Reddy [21]. Finally, the global material stiffness matrix is used to compute the fundamental nucleus $\boldsymbol{k_0^{ij\tau s}}$, then the global stiffness array $\boldsymbol{K}$ is assembled, and the stochastic structural response is obtained.

NUMERICAL RESULTS

In this work, a four layered balanced and symmetric VAT plate is studied. A compressive pressure $P = 7.75$ kPa is applied at one of the edges, while the opposite edge is clamped. The remaining two edges are free to deform. The fiber orientation considered is $\theta = [0\pm< 45{,}0 >]_s$, according to the notation introduced by Gürdal and Olmedo [22]. The elastic material properties are enlisted in Table I. Note that since a multiscale procedure is considered, fiber and matrix constituents are shown separately. The homogenized properties of the composite material when $V_f = 0.60$ are reported in Table I too.

Table I. Elastic properties of the constituents of the composite material and homogenized material properties for a fiber volume fraction $V_f = 0.60$. Longitudinal, transverse and shear modulus are expressed in GPa.

Constituent	$\boldsymbol{E_{11}}$	$\boldsymbol{E_{22}}$	$\boldsymbol{G_{12}}$	$\boldsymbol{G_{23}}$	$\boldsymbol{\nu_{12}}$	$\boldsymbol{\nu_{23}}$
Fiber	235.0	14.0	28.0	5.60	0.20	0.25
Matrix	4.80	4.80	1.79	1.79	0.34	0.34
$V_f = 0.60$	143.17	9.64	6.09	3.12	0.252	0.349

Once the material properties and boundary conditions were set, and after verifying the present numerical model against commercial software ABAQUS [23], a mesh convergence was carried out for both internal stress distribution and buckling loads. The mesh was chosen so that a good balance between accuracy and computational time was achieved since the latter influences the duration of the MC analysis.

STOCHASTIC MULTISCALE STRESS RESULTS

In this section, the microscale stress state is analyzed. Particularly, the location of the point of interest, referred to as point Q, is $Q \equiv (0{,}0{,}-h/2)$. The micromechanics stress state is retrieved by imposing the macroscale strain tensor and the FVF at point Q for each analysis. An example of the local stress field recovery is shown in

Figure 3. In it, the stresses over the fiber and transverse shear are represented. As expected, both the fiber and matrix present longitudinal compressive stresses. Moreover, and due to the

differences in the elastic properties of the components, a notable difference concerning the order of magnitude between the stresses at the fiber and the matrix regions is appreciated.

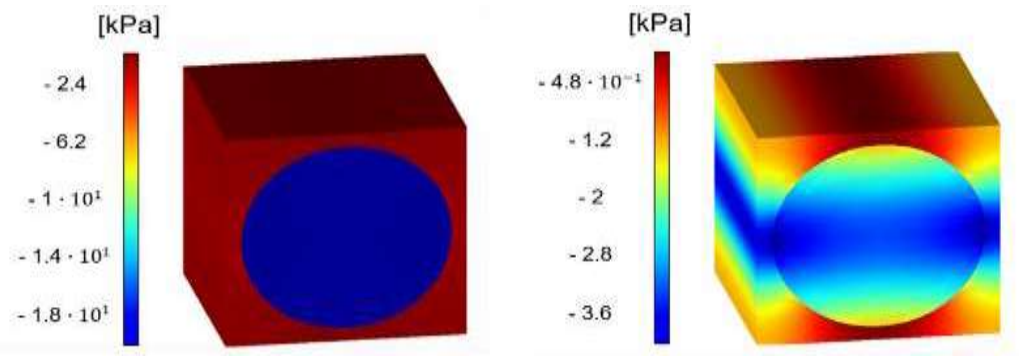

Figure 3. Local stress field recovery. σ_{11} (left) and σ_{12} (right).

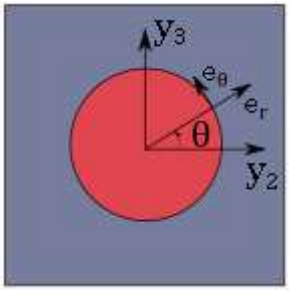

Figure 4. Representation of the cartesian and cylindrical reference frames at the RUC

Then, the micro stress tensor is rotated into a cylindrical coordinate system, represented in Figure 4, to show the distribution of stresses in the vicinities of the fiber-matrix interface. Note that the Cartesian longitudinal axis (y_1) coincides with the longitudinal axis of the cylindrical reference frame. For the sake of brevity, the rotation matrix between cartesian and cylindrical reference frames is omitted but can be found in the book by Lekhnitskii [24].

The local stress distribution over the fiber domain is represented in Figure 5. The axial stress σ_{11} is practically constant over the arc length and in perfect agreement with the stress distribution shown in Figure 3‘s left panel. Radial and circumferential shear stresses are also illustrated and show a symmetric and antisymmetric stress distribution, respectively. On the one hand, shear stresses do not present a large variability, as the shaded blue region in Figure 5 shows. On the other hand, the longitudinal stress distribution presents a variability up to ± 3 kPa. However, and for all the local stress tensor components, a narrow 95% confidence interval is appreciated. These values, evaluated at point Q and local circumferential coordinate $\theta = \pi/4$, are enlisted in Table II. The vast COV presented by σ_{r1} is due to the low mean value.

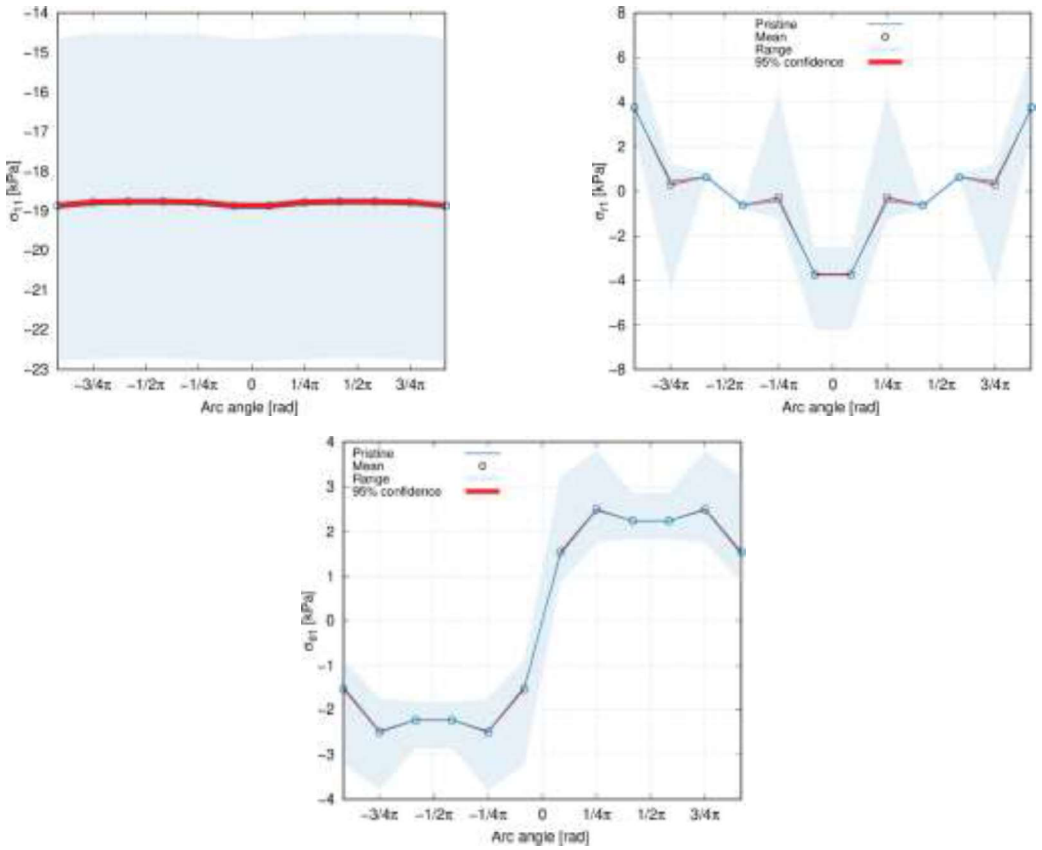

Figure 5. Representation of the fiber local stresses in the cylindrical reference system. Axial stress σ_{11} (left on top), and shear stresses σ_{r1} (right on top) and $\sigma_{\theta 1}$(bottom).

Table II. Microscale stress statistics at point Q and local coordinate $\theta = \pi/4$ over the fiber domain.

	Mean value	COV [%]	95% C.I.	Min-max range
σ_{11} [kPa]	-18.78	6.48	[-18.86,-18.71]	[-22.74,-14.53]
σ_{rr} [kPa]	-0.37	13.94	[-0.369,-0.363]	[-0.498,-0.148]
$\sigma_{\theta\theta}$ [kPa]	-0.48	5.07	[-0.481,-0.478]	[-0.547,-0.388]
$\sigma_{r\theta}$ [kPa]	0.91	6.14	[0.911,0.918]	[0.771,1.183]
σ_{r1} [kPa]	-0.29	221.68	[-0.33,-0.25]	[-1.24,4.36]
$\sigma_{\theta 1}$ [kPa]	2.50	11.23	[2.48,2.52]	[1.76,3.79]

STOCHASTIC BUCKLING RESPONSE

After computation of the internal stress state, one can calculate the geometric stiffness matrix and solve the buckling eigenvalue problem as depicted in [13]. The first six nominal buckling loads are enlisted in Table III.

Table III. Nominal buckling loads of the plates without defects.

F_{cr1} [N]	F_{cr2} [N]	F_{cr3} [N]	F_{cr4} [N]	F_{cr5} [N]	F_{cr6} [N]
143.59	159.08	216.77	310.22	366.45	407.53

The variability in the buckling loads due to the stochastic fiber volume fraction fields is reported in Table IV and Table V. Additionally, the mean value and COV are computed through the Monte Carlo outcomes and first- and second-order PCE in these tables.

Table IV. Mean buckling loads of the defective plates.

Critical load	Monte Carlo mean [N]	1st PCE mean [N]	2nd PCE mean [N]
F_{cr1}	143.48	143.48	143.49
F_{cr2}	159.21	159.21	159.21
F_{cr3}	217.16	217.16	217.16
F_{cr4}	310.21	310.46	310.48
F_{cr5}	366.45	366.61	366.62
F_{cr6}	407.53	407.91	407.93

Table V. Buckling loads' COV for the defective plates.

Critical load	Monte Carlo COV [%]	1st PCE COV [%]	2nd PCE COV [%]
F_{cr1}	3.14	3.16	3.16
F_{cr2}	3.07	3.08	3.09
F_{cr3}	3.20	3.22	3.21
F_{cr4}	3.11	3.12	3.12
F_{cr5}	3.27	3.31	3.31
F_{cr6}	3.11	3.11	3.10

A graphical representation of the statistical moments shown in the tables above is available in Figure 6.

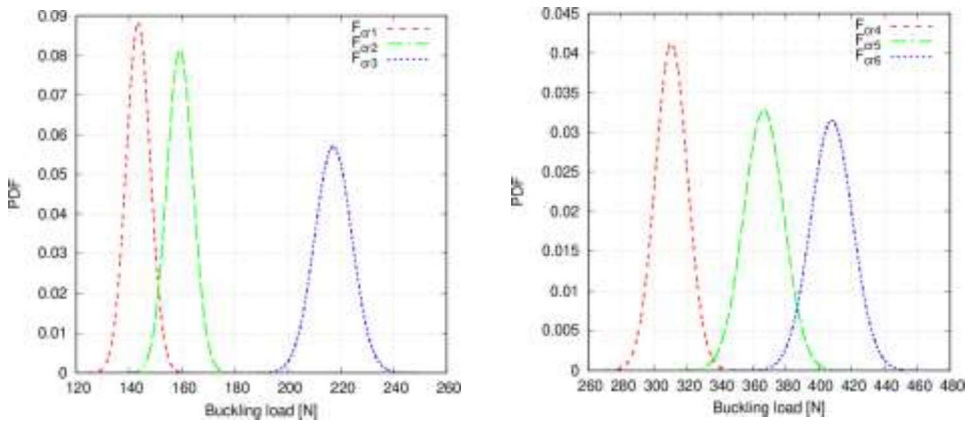

Figure 6. Representation of the first six buckling load PDFs.

From Figure 6, it is appreciated that overlapping PDF tails appear for the first and second buckling loads in the vicinities of 150 N. Such overlaps are also present between the fourth, fifth and sixth buckling loads. It is not known beforehand if this phenomenon implies mode switching. To shed some light, Modal Assurance Criterion (MAC) matrix is computed for each Monte Carlo sample with the following expression:

$$\mathrm{MAC}_{j,k}^{(i)} = \frac{|\phi_{i,j}^T \phi_{ref,k}|^2}{||\phi_{i,j}^T \phi_{i,j}|\,|\phi_{ref,k} \phi_{ref,k}|} \tag{6}$$

in which $\phi_{i,j}$ is the i-th sample of the j-th eigenvector, $\phi_{ref,k}$ refers to the k-th eigenvector of the reference solution and $\mathrm{MAC}_{j,k}^{(i)}$ denotes the i-th sample of the j,k component of the MAC matrix. The mean value and standard deviation of each term of the MAC matrix are computed and represented in a 3D plot in Figure 7. It can be inferred that no mode switching occurs since all the terms in the main diagonal of the matrix have a mean value close to one. Nevertheless, some out-of-the-diagonal components present non-zero values. This occurs because the defective modes have resemblances with the pristine ones.

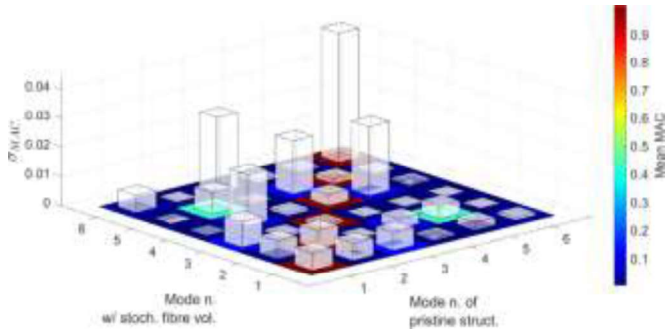

Figure 7. 3D representation of the MAC matrix.

CONCLUSIONS

In this manuscript, a multiscale methodology to study the influence of spatially varying FVF over VAT plates has been devised. In it, the spatial variation of FVF is introduced into the FE by means of stochastic fields generated with KLE. Therefore, a non-intrusive way of considering defects was achieved. Such defects are propagated through the different scales, and the structural response of the plate is retrieved.

Regarding the pre-buckling stress state, significant variability in the macroscale stresses is obtained, especially for the in-plane stress tensor components, which is due to the compressive state the plate is subjected to. The microscale stress tensor was then retrieved. For the studied point of interest, small variability in the stress distribution was obtained, but for the longitudinal stress. Additionally, narrow 95% confidence intervals were reported.

Concerning the buckling performance, it has been demonstrated that FVF affects the value of the buckling load. Indeed, a buckling load COV of around 3% has been found. This means that, in a 3σ reliability analysis, such critical loads may vary up to roughly 10% when microscale uncertainty is considered. Additionally, no mode switching has been appreciated, as demonstrated by the MAC matrix statistics. Nevertheless, the defective modes have shown resemblances with the pristine buckling modes.

Future works will focus on the consideration of these uncertainty procedures in the optimization of VAT structures and the development of micromechanical models for curved RUCs.

REFERENCES

1] Heinecke, F., and C. Willberg. 2019. "Manufacturing-induced imperfections in composite parts manufactured via automated fiber placement.," *Journal of Composite Science,* 3(2), 56.

2] Dey, S., T. Mukhopadhyay and S. Adhikari. 2015. "Stochastic free vibration analysis of angle-ply composite plates: A RS-HDMR approach.," *Composite Structures,* 122: 526:536

3] Sudret, B. and A. Der-Kiureghian. 2000. "Stochastic finite element methods and reliability.," Universitiy of California, Berkeley.

4] Ghanem, R. and P. Spanos. 1991. *Stochastic finite elements: a spectral approach.* New York: Springer International Publishing.

5] Guimaraes, T., H. Silva, D. Rade and C. Cesnik. 2020. "Aerolastic stability of conventional and tow-steered composite plates under stochastic fiber volume.," *AIAA Journal,* 58(6): 2748-2459.

6] Huang, S., S. Mahadevan and R. Rebba. 2007. "Collocation-based stochastic finite element analysis for random field problems" *Probabilistic Engineering Mechanics,* 22(2): 194-205.

7] Carrera, E., M. Cinefra, M. Petrolo and E. Zappino. 2014. *Finite Element Analysis of structures through Unified Formulation.* Wiley & Sons.

8] de Miguel, A., A. Pagani, W. Yu and E. Carrera. 2017. "Micromechanics of periodically heterogeneous materials using higher-order beam theories and the mechanics of structure genome," *Composite Structures,* 180: 484-496

9] Carrera, E., and M. Filippi. 2016. "A refined one-dimensional rotordynamics model with three-dimensional capabilities.," *Journal of Sound and Vibration,* 366: 343-356.

10] Cinefra, M., M. Petrolo, G. Li and E. Carrera. 2017. "Variable kinematic shell elements for composite laminates accounting for hygrothermal effects," *Journal of Thermal Stresses,* vol. 40(12): 1523-1544.

11] Vescovini, R., and L. Dozio. 2016. "A variable-kinematic model for variable stiffness plates: vibration and buckling analysis," *Composite Structures,* 142: 15-26.

12] Viglietti, A., E. Zappino and E. Carrera. 2019. "Analysis of variable angle tow composites structures using variable kinematics models," *Composites Part B: Engineering,* 171: 272-283.

Pagani, A., and A. Sanchez-Majano. 2020. "Influence of fiber misalignments on buckling performance of
13] variable stiffness composites using layerwise models and random fields," *Mechanics of Advanced Materials and Structures,* 1:16

Pagani, A., and A. Sanchez-Majano, 2021. "Stochastic stress analysis and failure onset of variables angle
14] tow laminates affected by spatial fibre variations.," *Composites Part C: Open Access,* 4: 100091

Gordon, W., and C. Hall. 1973. "Transfinite element methods: Blending-function interpolation over
15] arbitrary curved element domains," *Numerische Mathematik ,* 21: 109-129.

Wu, B., A. Pagani, W. Chen and E. Carrera. 2019. "Geometrically nonlinear refined shell theories by
16] Carrera Unified Formulation," *Mechanics of Advanced Materials and Structures,* 1-21.

Yu, W., and T. Tang. 2017. "Variational asymptotic method for unit cell homogenization of periodically
17] heterogeneous materials," *International Journal of Solids and Structures,* 44(11): 3738-3755.

Yu, W. 2016. "A unified theory for constitutive modeling of composites," *Journal of Mechanics of*
18] *Materials and Structures,* vol. 11(4): 1-32.

Betz,W., I. Papaioannou and D. Straub. 2014. "Numerical methods for the discretization of random fields
19] by means of the Karhunen–Loève expansion.," *Computer Methods in Applied Mechanics and Engineering,* 271: 109-129.

Marelli, S., and B. Sudret. 2019. " UQLab user manual -- Polynomial chaos expansions," ETH Zurich,
20] Zurich, Switzerland, Zurich.

Reddy, J.N. 2004. *Mechanics of laminated composite plates and shells: Theory and Analysis*, Boca Raton:
21] CRC Press.

Gürdal, Z., and R. Olmedo. 1993."In-plane response of laminates with spatially varying fiber orientations -
22] Variable stiffness concept," *AIAA Journal,* 31(4): 751-758.

Smith, M. 2009. *ABAQUS/Standard's User Manual, Version 6.9*, Dassault Systèmes Simulia Corp.
23]

Lekhnitskii, S. 1984. *Anisotropic plates.* New York: Gordon and Breach, Science Publishers.
24]